

Spin-current order in anisotropic triangular antiferromagnets

Andrey V. Chubukov¹ and Oleg A. Starykh²

¹Department of Physics, University of Wisconsin, Madison, WI 53706

²Department of Physics and Astronomy, University of Utah, Salt Lake City, UT 84112

(Dated: November 13, 2018)

We analyze instabilities of the collinear up-up-down state of a two-dimensional quantum spin- S spatially anisotropic triangular lattice antiferromagnet in a magnetic field. We find, within large- S approximation, that near the end point of the plateau, the collinear state becomes unstable due to condensation of two-magnon bound pairs rather than single magnons. The two-magnon instability leads to a novel 2D vector chiral phase with alternating spin currents but no magnetic order in the direction transverse to the field. This phase breaks a discrete Z_2 symmetry but preserves a continuous $U(1)$ one of rotations about the field axis. It possesses orbital antiferromagnetism and displays a magnetoelectric effect.

PACS numbers:

Introduction. The field of frustrated quantum magnetism has witnessed a remarkable revival of interest in recent years due to rapid progress in the fabrication and characterization of new materials and a multitude of theoretical ideas about competing orders and new quantum states of matter [1]. Studies of two-dimensional (2D) quantum triangular lattice antiferromagnets with spatially anisotropic exchange, such as Cs_2CuCl_4 and Cs_2CuBr_4 , are of particular interest because of their surprisingly rich phase diagrams in a magnetic field [2, 3] which includes novel quantum states which have no classical analogs and display a wealth of properties which are highly sought after for applications. The large number of different phases involved, which reaches 9 in the case of Cs_2CuBr_4 [3], reveals a highly complex interplay between quantum fluctuations and anisotropy of the interactions.

One of the best understood phases of a frustrated spin system in a magnetic field is a collinear state with a fixed, field-independent magnetization equal to exactly $1/3$ of the saturation value. In this state, known as the up-up-down (UUD), two spins in each triangle point up and one points down. This quantum state preserves continuous $U(1)$ symmetry of rotations about the field direction and has finite gaps in all spin excitations [4]. The UUD state is similar to plateau states in quantum Hall effect, although, unlike them, it spontaneously breaks lattice translational symmetry. An extension of the UUD state with unbroken translational symmetry has been proposed theoretically but not yet found experimentally [5, 6].

In a classical isotropic 2D Heisenberg systems with nearest exchange J , the UUD phase is the ground state for just one value of the external field $h = 3J$ ($1/3$ of the saturation field $h_{\text{sat}} = 9J$). At all other fields spins order in a non-collinear fashion. In an anisotropic lattice with exchanges J and J' (see Fig. 1), a non-collinear order wins for all fields, so that classically UUD phase is never a ground state. For quantum systems, the situation is different as quantum fluctuations favor a collinear spin structure and compete with classical fluctuations [4, 7, 8]. In the isotropic case, quantum fluctuations stabilize the UUD phase with gapped spin-wave excitations in a finite interval of h with the width of order $1/S$. In an anisotropic case, the width of the UUD phase is determined

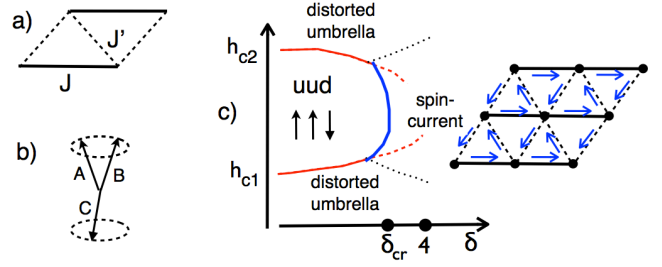


FIG. 1: (Color online) (a) Anisotropic triangular lattice with exchanges J and J' . (b) Distorted umbrella state. (c) Schematic phase diagram of the model in the vicinity of the UUD end-point at $\delta = 4$. Thin solid (red) lines mark single-particle instabilities of the UUD state at $h_{c1,c2}(\delta)$. Thick solid (blue) line is the two-particle instability line towards a spin-current state, which emerges at $\delta > \delta_{\text{cr}}$, and dotted (black) lines indicate phase transitions between the umbrella and the spin-current state. Dashed (red) line indicates a would-be single-particle instability, which is pre-empted by the two-particle instability. (Blue) arrows in the insert on the right show the arrangement of spin currents.

by the competition between $1/S$, which measures the strength of quantum fluctuations, and the degree of anisotropy of exchange interactions $(1 - J'/J)$ (Ref. [8]). The dimensionless parameter, which determines the UUD width relative to its value in the isotropic case, is $\delta = (40/3)S(1 - J'/J)^2$ (we use the same numerical factor as in [8]). The UUD phase persists up to a finite anisotropy $\delta_{\text{cr}} = 4$, see Fig. 1. The boundaries of the UUD phase have been determined from the local stability analysis [8] as the values of h at which spin-wave dispersion softens. Of the two low-energy spin-wave branches, one softens at the lower boundary of the UUD phase and another at the upper boundary. Near the critical J'/J , both spin-wave instabilities occur at finite momenta, and each leads to a chiral, non-coplanar state (often called a distorted umbrella), in which $\langle \mathbf{S}_r \rangle$ has finite components along both directions perpendicular to the field [8, 9] (see Fig. 1).

The analysis of the same model for $S = 1/2$, however, found very different states surrounding the UUD plateau near

its end point, which for $S = 1/2$ extends all way to $J' = 0$ [10]. These states are collinear spin-density wave (SDW) states, with incommensurate spin modulations along the field direction but *no* long-range order in the transverse direction [10]. This discrepancy poses the question whether the phase diagram for $S = 1/2$ is qualitatively different from the one at large S , or the ground states surrounding the UUD phase are different from the ones predicted by spin-wave theory even for large S .

In this work we re-visit the large S analysis of the UUD state and show that the spin-wave phase diagram is incomplete for *any* S . We show that, prior to a single-magnon instability, the system undergoes a pairing instability, in which the two-particle collective mode, made of magnons from the two low-energy branches, softens at zero total momentum of the pair. As a result, the actual instability near the end point of UUD phase is towards the uni-axial state with no magnetic order in the transverse direction, similar to the situation for $S = 1/2$. We solve the “gap” equation for the two-magnon order parameter and show that it is purely *imaginary*. Such order parameter breaks a discrete Z_2 symmetry and gives rise to a bond-nematic state with non-zero vector and scalar chiralities within a single triangle of spins: $\langle \mathbf{S}_A \cdot \mathbf{S}_B \times \mathbf{S}_C \rangle \neq 0$ and $\langle \mathbf{S}_A \times \mathbf{S}_B \rangle = \langle \mathbf{S}_B \times \mathbf{S}_C \rangle = \langle \mathbf{S}_C \times \mathbf{S}_A \rangle \neq 0$ (vector and scalar chiralities are proportional to each other since the total magnetization $M = \langle S_z \rangle$ is finite). Such a state supports circulating spin currents (Fig. 2) and we label it a *spin-current* state (SC). We present the modified large- S phase diagram of the model in Fig. 1.

Experimental signatures of a SC state are rather peculiar. First, it exhibits a magneto-electric effect because both spin current and electric field are odd under spatial reflections and couple linearly [12]. As a result, spin-wave excitations of the SC state depend linearly on E . Second, orbiting spin currents generate charge currents, which in turn produce staggered magnetic moments, which can be measured by NMR and μ SR [13].

The model. We consider a system of localized spins on an anisotropic triangular lattice with Heisenberg nearest-neighbor interactions J and J' , subject to an external field $\tilde{h} = 2\mu_B H_z$:

$$\mathcal{H} = \sum_{\mathbf{r}} \left(J \mathbf{S}_{\mathbf{r}} \mathbf{S}_{\mathbf{r}+\mathbf{a}_x} + J' \sum_{j=1,2} \mathbf{S}_{\mathbf{r}} \mathbf{S}_{\mathbf{r}+\mathbf{a}_j} - \tilde{h} S_{\mathbf{r}}^z \right), \quad (1)$$

where $\mathbf{a}_{1,2} = a(1/2, \pm\sqrt{3}/2)$ connects spins on neighboring chains, and a is the lattice constant. For convenience, we rescale $\tilde{h} = hS$ and use h for the field. The saturation field, above which the magnetization M reaches maximum possible value $M_{\text{sat}} = S$, is given by $h_{\text{sat}} = (2J + J')^2/J$. We are interested in the behavior of the system near $h_{\text{sat}}/3$, where quantum fluctuations win over classical fluctuations and stabilize UUD phase in a finite range of fields. In the isotropic case, $J' = J$, the UUD phase exists in a field range between $h_{c1} = (h_{\text{sat}}/3)(1 - 0.5/2S)$ and $h_{c2} = (h_{\text{sat}}/3)(1 + 1.3/2S)$. In the anisotropic case, $J' < J$, the width of the UUD state

decreases and eventually vanishes at $\delta_{\text{cr}} = 4$, which defines $J'_{\text{cr}} = J(1 - \sqrt{3}/10S)$

The excitation spectrum of the UUD phase at $\delta \leq 4$ can be straightforwardly obtained by using a three-sublattice representation for two spin-up and one spin-down sublattices and introducing [8, 11] three sets of Holstein-Primakoff bosons, a, b , and c . One of the three spin-wave branches describes the precession of the total magnetization, has energy of the order $h_{\text{sat}}/3$, and is irrelevant to our analysis. The other two branches, denoted $d_{1(2),\mathbf{k}}$ below, describe low-energy excitations. Explicitly,

$$\mathcal{H}_{\text{uud}}^{(2)} = S \sum_{\mathbf{k}} \left(\omega_1 d_{1,\mathbf{k}}^\dagger d_{1,\mathbf{k}} + \omega_2 d_{2,\mathbf{k}}^\dagger d_{2,\mathbf{k}} \right), \quad (2)$$

where at small \mathbf{k}

$$\omega_{1,2}(\mathbf{k}) = \pm \left(h - h_0 - \frac{1}{5S}J - \frac{3}{4}J\mathbf{k}^2 \right) + \frac{3J}{20S}Z_{\mathbf{k}}, \quad (3)$$

$$Z_{\mathbf{k}} = \sqrt{9 + 10S(6\mathbf{k}^2 - 3\delta k_x^2 + 10S\mathbf{k}^4)}, \quad (4)$$

and $h_0 = J + 2J'$. The excitation $d_{1,\mathbf{k}}$ softens at the lower boundary of the UUD phase, at $h = h_{c1}(\delta) = h_{\text{end}} - 9J/(40S)\sqrt{(4-\delta)/3}$, where $h_{\text{end}} = h_0(1 + 17/(120S))$. The softening happens at a finite momenta $\pm\mathbf{k}_1 = (\pm k_1, 0)$, where $k_1 \approx (3/(10S))^{1/2}(1 + \sqrt{(4-\delta)/12})$. The excitation $d_{2,\mathbf{k}}$ softens at the upper boundary $h = h_{c2}(\delta) = h_{\text{end}} + 27J/(40S)\sqrt{(4-\delta)/3}$, at momenta $\pm\mathbf{k}_2 = (\pm k_2, 0)$, where $k_2 = (3/(10S))^{1/2}(1 - \sqrt{(4-\delta)/12})$. The spin-wave softening at either $h_{c1}(\delta)$ or $h_{c2}(\delta)$ signals condensation of one-magnon excitations. A Ginzburg-Landau-type analysis shows [8] that condensation spontaneously breaks Z_2 symmetry between degenerate minima at $\pm\mathbf{k}_1$ and $\pm\mathbf{k}_2$. As a result, one-magnon condensation gives rise to an incommensurate spiral order with spontaneously broken $O(2) \times Z_2$ symmetry and a finite non-coplanar long-range order $\langle S_{\mathbf{r}}^{x,y} \rangle \neq 0$.

At the end-point of the plateau $\delta = 4$, $h_{c1} = h_{c2} = h_{\text{end}}$, both spin-wave branches touch zero simultaneously at $\pm\mathbf{k}_0 = (\pm k_0, 0)$, where $k_0 = \sqrt{3/(10S)}$. The presence of four soft modes leads to a variety of possible non-coplanar chiral orders with non-zero $\langle S_{\mathbf{r}}^{x,y} \rangle$. However, we show below that instead the system undergoes a pre-emptive pairing instability into a state with no transverse order, $\langle S_{\mathbf{r}}^{x,y} \rangle = 0$, but nonetheless with a finite chirality $\langle \hat{z} \cdot \mathbf{S}_{\mathbf{r}} \times \mathbf{S}_{\mathbf{r}'} \rangle \neq 0$.

Magnon pairing. To analyze a possibility of a bound state of two magnons, we need to include magnon-magnon interaction. The derivation of the interaction Hamiltonian is lengthy but straightforward: one has to express two-magnon interaction Hamiltonian $\mathcal{H}_{\text{uud}}^{(4)}$, originally written in terms of $a_{\mathbf{k}}, b_{\mathbf{k}}$ and $c_{\mathbf{k}}$ bosons, in terms of the low-energy eigen-modes $d_{1,\mathbf{k}}$ and $d_{2,\mathbf{k}}$ from Eq. (2). The full transformation is given in [11]. Near momenta $\pm\mathbf{k}_0$, which are mostly relevant to the

pairing problem, this transformation simplifies to

$$\begin{aligned} a_{\mathbf{k}} &= \frac{f(\mathbf{k})}{\sqrt{2}}(e^{is_{\mathbf{k}}}d_{1,\mathbf{k}} - e^{-is_{\mathbf{k}}}d_{2,-\mathbf{k}}^\dagger), \\ b_{\mathbf{k}} &= -\frac{f(\mathbf{k})}{\sqrt{2}}(e^{-is_{\mathbf{k}}}d_{1,\mathbf{k}} + e^{is_{\mathbf{k}}}d_{2,-\mathbf{k}}^\dagger), \\ c_{\mathbf{k}} &= f(\mathbf{k})(d_{2,\mathbf{k}} - e^{i2s_{\mathbf{k}}}d_{1,-\mathbf{k}}^\dagger). \end{aligned} \quad (5)$$

where $f(\mathbf{k}) = \sqrt{k_0}[(k_x \pm k_0)^2 + k_y^2 + (1 - \delta/4)k_0^2]^{-1/4}$ and $s_{\mathbf{k}} = \pi \text{sign}(k_x)/4$.

Consider first $\delta < 4$, when only one boson becomes soft at either h_{c1} or h_{c2} , while other remains massive and can be neglected. For concreteness, consider the vicinity of h_{c1} , where d_1 excitation softens. The magnon-magnon pairing interaction involving only d_1 bosons is

$$\mathcal{H}_{d_1 d_1}^{(4)} = \frac{8(J + 2J')}{(4 - \delta)} \frac{3}{N} \sum_{p,q} d_{1,\mathbf{k}_1+\mathbf{p}}^\dagger d_{1,-\mathbf{k}_1-\mathbf{p}}^\dagger d_{1,\mathbf{k}_1+\mathbf{q}} d_{1,-\mathbf{k}_1-\mathbf{q}} \quad (6)$$

This interaction is obviously strongly repulsive and does not give rise to a bound state. The same holds for d_2 mode near h_{c2} . As a result, one-magnon condensations at h_{c1} and h_{c2} are the true instabilities, and the system develops a non-coplanar spiral order at $h \geq h_{c2}$ and $h \leq h_{c1}$.

For $\delta \approx 4$, the situation is different. Magnon-magnon interactions within d_1 or d_2 sectors are still repulsive, but now we also have interaction between d_1 and d_2 bosons, both of which are gapless at $\pm \mathbf{k}_0$. The $d_1 - d_2$ interaction with zero total momentum has two relevant terms: one describes "normal" $2 \rightarrow 2$ process with simultaneous creation and annihilation of d_1 and d_2 bosons, the other describes "anomalous" $4 \rightarrow 0$ and $0 \rightarrow 4$ processes with simultaneous creation or annihilation of two d_1 and two d_2 bosons. We find that the strongest pairing interaction involves momentum transfer $\pm 2\mathbf{k}_0$ for each of the bosons involved. The corresponding interaction reads

$$\begin{aligned} \mathcal{H}_{d_1 d_2}^{(4)} &= \frac{3}{N} \sum_{p,q} \Phi(p, q) \left(d_{1,\mathbf{k}_0+\mathbf{p}}^\dagger d_{2,-\mathbf{k}_0-\mathbf{p}}^\dagger d_{1,-\mathbf{k}_0+\mathbf{q}} d_{2,\mathbf{k}_0-\mathbf{q}} \right. \\ &\quad \left. - d_{1,\mathbf{k}_0+\mathbf{p}}^\dagger d_{2,-\mathbf{k}_0-\mathbf{p}}^\dagger d_{1,-\mathbf{k}_0+\mathbf{q}}^\dagger d_{2,\mathbf{k}_0-\mathbf{q}} \right) + \text{h.c.} \end{aligned} \quad (7)$$

where p and q are much smaller than k_0 , and the vertex

$$\Phi(p, q) = -(J + 2J')f^2(p)f^2(q) \rightarrow -(J + 2J')\frac{k_0^2}{|\mathbf{p}||\mathbf{q}|} \quad (8)$$

where $f(p)$ was introduced after Eq. (5), and the limit stands for $\delta \rightarrow 4$. The pairing interaction with small momentum transfer, $\tilde{\Phi}(p, q)d_{1,\mathbf{k}_0+\mathbf{p}}^\dagger d_{2,-\mathbf{k}_0-\mathbf{p}}^\dagger d_{1,\mathbf{k}_0+\mathbf{q}} d_{2,-\mathbf{k}_0-\mathbf{q}}$, has a much smaller $\tilde{\Phi}(p, q)$ which remains finite in the limit $p, q \rightarrow 0$. Such interaction is then irrelevant for our analysis.

Now observe that the sign of $2 \rightarrow 2$ term is negative, while the one of $4 \rightarrow 0$ term is positive. The negative sign of the $2 \rightarrow 2$ term implies that the "normal" interaction between d_1 and d_2 bosons is attractive and favors a pairing with

$$\begin{aligned} F_{\mathbf{k}_0}(p) &= \langle d_{1,\mathbf{k}_0+\mathbf{p}} d_{2,-\mathbf{k}_0-\mathbf{p}} \rangle = F_{-\mathbf{k}_0}(p) = \\ &= \frac{\tilde{\Upsilon} f^2(\mathbf{p})}{\omega_1(\mathbf{k}_0 + \mathbf{p}) + \omega_2(\mathbf{k}_0 + \mathbf{p})} \rightarrow \frac{\tilde{\Upsilon}}{p^2}. \end{aligned} \quad (9)$$

The positive sign of the $4 \rightarrow 0$ term does not allow the solution with real $\tilde{\Upsilon}$ (the corresponding coupling constant vanishes), but instead favors a solution with imaginary $\tilde{\Upsilon} = i\Upsilon$. For such solution the pairing vertex which couples to $4 \rightarrow 0$ term has opposite sign compared to the vertex which couples to $2 \rightarrow 2$ term, and this extra sign change compensates the sign difference between $2 \rightarrow 2$ and $4 \rightarrow 0$ interactions. Note that since the Hamiltonian (7) does not conserve the number of bosons, the order parameter does not possess a $U(1)$ phase symmetry. In practice, this implies that the gap equations for real and imaginary Υ 's are different. And, in fact, the symmetry that is spontaneously broken at the transition is Z_2 , corresponding to the sign of Υ .

For $\tilde{\Upsilon} = i\Upsilon$, the linearized "gap" equation reads at $\delta = 4$,

$$\Upsilon = \frac{6\Upsilon}{NS} \sum_p \frac{(J + 2J')k_0^2}{p^2} \frac{1}{\omega_1(\mathbf{k}_0 + \mathbf{p}) + \omega_2(\mathbf{k}_0 + \mathbf{p})}. \quad (10)$$

Substituting the dispersions, we find

$$1 = \frac{1}{S} \frac{3}{N} \sum_p \frac{k_0}{|\mathbf{p}|^3}. \quad (11)$$

It is important that the integrand scales as $1/|\mathbf{p}|^3$, so that the 2D integral over \mathbf{p} diverges and overcomes the smallness of $1/S$ in the pre-factor. In $1/|\mathbf{p}|^3$, one power of $1/|\mathbf{p}|$ comes from the dispersion and the other two powers are due to the divergence of the coherence factor $f(p)$ at $p \rightarrow 0$. Away from $\delta = 4$, $|\mathbf{p}|$ is replaced by $(|\mathbf{p}|^2 + (1 - \delta/4)k_0^2)^{1/2}$, and the integral in the r.h.s of (11) behaves as $1/\sqrt{4 - \delta}$. Collecting powers of $1/S$, we find that a nonzero Υ emerges at $\delta_{\text{cr}} = 4 - O(1/S^2)$.

For completeness, we also analyzed possible pairing with the total momentum $\pm 2\mathbf{k}_0$, but found that there is no enhancement of the kernel of the gap equation by coherence factors and, hence, no instability at large S .

Spin-current order. The two-magnon instability does not lead to a conventional spin order in the direction perpendicular to the field because $\langle d_{1,k} \rangle = \langle d_{2,k} \rangle = 0$. $F_{\mathbf{k}_0}(p) \sim \Upsilon$ does not lead to modulations of $S_{\mathbf{r}}^z$ or the bond order because the condensate does not contribute to magnon density or to $\langle \mathbf{S}_A \cdot \mathbf{S}_B \rangle$ [11]. However, one can easily verify that for each triangle we now have $\langle \hat{z} \cdot \mathbf{S}_A \times \mathbf{S}_C \rangle = \langle \hat{z} \cdot \mathbf{S}_C \times \mathbf{S}_B \rangle = \langle \hat{z} \cdot \mathbf{S}_B \times \mathbf{S}_A \rangle \propto \Upsilon$, which implies a finite vector chirality and orbital spin currents which run in opposite directions in neighboring triangles, Figure 2. Note that the sign of Ising order parameter Υ determines the sense of spin current circulation. In our case vector chirality generates a non-zero scalar chirality $\langle \mathbf{S}_A \cdot \mathbf{S}_B \times \mathbf{S}_C \rangle \sim \Upsilon$ as well, because of the finite magnetization M along the z (magnetic field) axis. For triangles separated by distance \mathbf{r} , $\hat{z} \cdot \langle \mathbf{S}(0) \times \mathbf{S}(\mathbf{r}) \rangle$ scales as $\Upsilon \cos(\mathbf{k}_0 \mathbf{r}) e^{-r k_0 \sqrt{1 - \delta/4}}$ [11].

A spin-current (SC) order in dimensions $D > 1$ is normally associated with non-coplanar spin ordering when the spins spontaneously select the direction of rotation in the XY

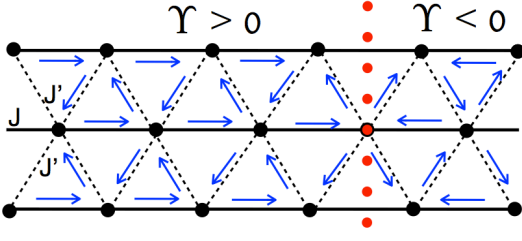


FIG. 2: (Color online) The structure of spin currents in the SC state. The domain wall, denoted by vertical (red) dotted line, separates domains with opposite chirality Υ .

plane. Remarkably, in our case the SC order appears in the absence of the standard spin order in the XY plane.

The emergence of the SC order can be thought of as spontaneous generation of Dzyaloshinskii-Moria (DM) interaction. Indeed, the interaction Hamiltonian (7) can be written as $\mathcal{H}_{d_1 d_2}^{(4)} = -(9J/N)\mathcal{H}_{k_0}^{\text{DM}}\mathcal{H}_{-k_0}^{\text{DM}}$, where [11]

$$\begin{aligned}\mathcal{H}_{\pm k_0}^{\text{DM}} &= \frac{1}{6S} \sum_r \hat{z} \cdot \mathbf{S}_r \times (\mathbf{S}_{r+\mathbf{a}_1} + \mathbf{S}_{r+\mathbf{a}_2}) \\ &= i \sum_{\mathbf{k} \in \pm \mathbf{k}_0} f_k^2 \left(d_{1,\mathbf{k}} d_{2,-\mathbf{k}} - d_{1,\mathbf{k}}^\dagger d_{2,-\mathbf{k}}^\dagger \right).\end{aligned}\quad (12)$$

As a result, the development of a non-zero Υ can be viewed as the appearance of Dzyaloshinskii-Moria interaction $D(\mathcal{H}_{k_0}^{\text{DM}} + \mathcal{H}_{-k_0}^{\text{DM}})$, with $D \sim \Upsilon$. This observation helps to understand magneto-electric effect in the SC state: because D is a pseudoscalar, it couples linearly to an electric field E , i.e., $D = D_0 + D_1 E + \dots$. As a result, spin-wave excitations of the SC phase depend linearly on E .

SC order has been previously explored in 1D spin ladders [14–16] and was suggested for a frustrated Heisenberg model in 2D [17, 18]. There, however, a SC state is a spiral state, in which a continuous $U(1)$ symmetry is restored by strong quantum fluctuations [18]. In our case spiral states are present in the phase diagram away from the end-point of the UUD phase, while the SC state emerges as a result of a pre-emptive two-magnon instability rather than due to divergent one-magnon fluctuations. Our two-magnon instability (which necessary leads to an imaginary order parameter) is also fundamentally different from two-magnon instabilities with real order parameter which lead to a spin-nematic order, either on a site or on a bond [19–24]. Such order generally occurs in systems with ferromagnetic exchanges at least on some of the bonds, when there is an attractive interaction between magnons. Here, all exchange couplings are antiferromagnetic, and magnon-magnon interaction is repulsive. Our pairing of magnons from different branches is conceptually similar to the inter-pocket pairing in multi-band fermionic systems, such as Fe-based superconductors with only electron pockets [25].

The phase diagram near the end point of UUD state has been recently analyzed in [9] in a self-consistent semiclassical formalism. This method, however, does not allow for the analysis of two-particle instabilities.

Comparison with SDW state. Although our analysis uses $1/S$ expansion, it is nevertheless instructive to compare symmetry properties of our spin-current state with that of a collinear SDW state observed for $S = 1/2$ near the end point of the UUD phase. Like we said, spin-current state is much closer to SDW state than a spiral state (the result of one-magnon condensation) because both spin-current and SDW states preserve $U(1)$ symmetry of rotations about the field direction. But the two states do differ as SDW state has no chiral order [10]. It may be that $S = 1/2$ is simply special and non-chiral SDW state is only present at $S = 1/2$. But it also may be that the two-magnon instability, which we found, is only a ‘tip of the iceberg’, and the two-magnon condensation triggers the development of multi-magnon condensates at some $\delta > \delta_{\text{cr}}$, which in turn changes the properties of the spin-current state. This last possibility is inspired by the observation that SDW state is incommensurate and that the UUD-SDW transition for $S = 1/2$ is a commensurate-incommensurate transition [10]. Such transition occurs via a proliferation of solitons – strings of displaced spins which are shifted from their equilibrium UUD pattern. Since changing the direction of a single spin S requires $2S$ magnons, a proliferation of solitons implies condensation of $2S$ magnons per every displaced spin. Then, in magnon description, a commensurate-incommensurate transition involves a condensation of an infinite number of magnons. One can imagine, by analogy with coupled superconducting and spin density orders [26], that proliferation of SC domain walls, depicted in Fig. 2, may cause the appearance of an incommensurate modulation of $\langle S^z \rangle$ due to “density-density” type coupling between the magnon density and the density of domain walls. Whether or not this is the case requires going beyond the instability condition (11) and analyzing excitation spectrum and inter-pair interactions within the spin-current phase [27].

Conclusions. We have described a novel two-magnon pairing instability of the up-up-down phase of the spatially anisotropic triangular lattice antiferromagnet in a magnetic field. The magnon pairing is of “inter-band” type in that the condensate is made out of bosons from the two different spin-wave branches. This instability pre-empt a single-magnon condensation for arbitrary spin S and gives rise to a highly unconventional 2D order in which transverse spin components are disordered, yet the ground state has a non-zero vector chirality on every lattice bond and circulating spin currents in every elementary triangle. This state breaks Z_2 chiral symmetry but preserves $U(1)$ symmetry of rotations about the field direction. The development of such a phase can be thought of as a spontaneous generation of the Dzyaloshinskii-Moriya interaction. This new state exhibits a magneto-electric effect, which gives rise to a non-trivial linear dependence of spin-wave excitations on the applied electric field E , and also has staggered magnetic moments, which can be measured by NMR and μSR .

We acknowledge illuminating discussions with L. Balents, C. Batista, A. Daley, L. Glazman, A. Furusaki, O. Kolezhuk, and O. Sushkov. We thank Qi Hu for pointing out inconsis-

tencies in Eq.(9) and in several related formulas in the supplementary part of the paper. This work was supported by DOE DE-FG02-ER46900 (A.V.Ch.) and by NSF DMR-1206774 (O.A.S.).

-
- [1] L. Balents, *Nature* **464**, 199 (2010).
 - [2] Y. Tokiwa, T. Radu, R. Coldea, H. Wilhelm, Z. Tylczynski, and F. Steglich, *Phys. Rev. B* **73**, 134414 (2006).
 - [3] N. Fortune, S. Hannahs, Y. Yoshida, T. E. Sherline, Y. Takano, T. Ono, and H. Tanaka, *Phys. Rev. Lett.* **102**, 257201 (2009).
 - [4] A. V. Chubukov and D. I. Golosov, *J. Phys.: Condens. Matter* **3**, 69 (1991).
 - [5] G. Misguich, Th. Jolicoeur, and S. M. Girvin, *Phys. Rev. Lett.* **87**, 097203 (2001).
 - [6] J. Alicea and M. P. A. Fisher, *Phys. Rev. B* **75**, 144411 (2007).
 - [7] C. Griset, S. Head, J. Alicea, O. A. Starykh, *Phys. Rev. B* **84**, 245108 (2011).
 - [8] J. Alicea, A. V. Chubukov, and O. A. Starykh, *Phys. Rev. Lett.* **102**, 137201 (2009).
 - [9] T. Coletta, M. E. Zhitomirsky, and F. Mila, *Phys. Rev. B* **87**, 060407(R) (2013).
 - [10] R. Chen, H. Ju, H. C. Jiang, O. A. Starykh, and L. Balents, *Phys. Rev. B* **87**, 165123 (2013).
 - [11] See Supplementary Material for more details.
 - [12] H. Katsura, N. Nagaosa, and A. V. Balatsky, *Phys. Rev. Lett.* **95**, 057205 (2005); M. Mostovoy, *Phys. Rev. Lett.* **96**, 067601 (2006).
 - [13] K. A. Al-Hassanieh, C. D. Batista, G. Ortiz, and L. N. Bulaevskii, *Phys. Rev. Lett.* **103**, 216402 (2009).
 - [14] A. A. Nersisyan, A. O. Gogolin, F. H. L. Essler, *Phys. Rev. Lett.* **81**, 910 (1998).
 - [15] A. Kolezhuk and T. Vekua, *Phys. Rev. B* **72**, 094424 (2005).
 - [16] T. Hikihara, T. Momoi, A. Furusaki, and H. Kawamura, *Phys. Rev. B* **81**, 224433 (2010).
 - [17] P. Chandra, P. Coleman, and A.I. Larkin, *J. Phys.: Condens. Matter* **2**, 7933 (1990).
 - [18] A. Läuchli, J.C. Domenge, C. Lhuillier, P. Sindzingre, and M. Troyer, *Phys. Rev. Lett.* **95**, 137206 (2005).
 - [19] A. F. Andreev and I. A. Grishchuk, *Sov. Phys. JETP* **60**, 267 (1984).
 - [20] A. V. Chubukov, *Phys. Rev. B* **43**, 3337 (1991).
 - [21] T. Hikihara, L. Kecke, T. Momoi, and A. Furusaki, *Phys. Rev. B* **78**, 144404 (2008).
 - [22] J. Sudan, A. Lüscher, and A. Läuchli, *Phys. Rev. B* **80**, 140402(R) (2009).
 - [23] M. E. Zhitomirsky and H. Tsunetsugu, *Europhys. Lett.* **92**, 37001 (2010).
 - [24] A. V. Sizanov and A. V. Syromyatnikov, *JETP Lett.* **97**, 114 (2013).
 - [25] I. I. Mazin, *Phys. Rev. B* **84**, 024529 (2011), M. Khodas and A. V. Chubukov, *Phys. Rev. Lett.* **108**, 247003 (2012).
 - [26] E. Demler, S. Sachdev, Y. Zhang, *Phys. Rev. Lett.* **87**, 067202 (2001).
 - [27] P. Nozieres and D. Saint James, *J. Physique*, **43**, 1133 (1982); L. Radzihovsky, P. B. Weichman, J. I. Park, *Annals of Physics* **323**, 2376 (2008).

SUPPLEMENTARY MATERIAL FOR “SPIN-CURRENT ORDER IN ANISOTROPIC TRIANGULAR ANTIFERROMAGNETS” BY A. V. CHUBUKOV AND O. A. STARYKH

One-magnon excitations in the UUD phase

One-magnon excitations in the UUD phase in the anisotropic case ($J' < J$) have been analyzed in Ref. 1. For completeness, we present here the details of the derivation. We will use some of intermediate formulas in the next section, when we derive the pairing interaction between magnons.

Spin-wave description of the UUD state proceeds as follows. First, we use a three-sublattice representation where spins point up on sublattices A and B and down on sublattice C, and introduce Holstein-Primakoff bosons a , b , and c respectively. Spins on the A sublattice are described by

$$S_A^z(\mathbf{r}) = S - a_{\mathbf{r}}^\dagger a_{\mathbf{r}},$$

$$S_A^+(\mathbf{r}) = \sqrt{2S} \sqrt{1 - \frac{a_{\mathbf{r}}^\dagger a_{\mathbf{r}}}{2S}} a_{\mathbf{r}} \approx \sqrt{2S} (1 - \frac{a_{\mathbf{r}}^\dagger a_{\mathbf{r}}}{4S}) a_{\mathbf{r}}, \quad (1)$$

and spins on the B sublattice are represented by the same expressions with $a_{\mathbf{r}}$ replaced by $b_{\mathbf{r}}$. The expansion of the square-root is valid for $S \gg 1$, and below we assume that S is indeed large. Spins on C sublattice points opposite to those on A and B sublattices, and we have

$$S_C^z(\mathbf{r}) = -S + c_{\mathbf{r}}^\dagger c_{\mathbf{r}}, \quad S_C^-(\mathbf{r}) = \sqrt{2S} (1 - \frac{c_{\mathbf{r}}^\dagger c_{\mathbf{r}}}{4S}) c_{\mathbf{r}}. \quad (2)$$

Plugging this in (1), we obtain spin-wave Hamiltonian as the sum of the linear (harmonic) term $H^{(2)}$ and the interaction terms $H^{(4)}$

$$H^{(2)} = S \sum_{\mathbf{k}} \left[\gamma_{\mathbf{k}} a_{\mathbf{k}}^\dagger b_{\mathbf{k}} + \gamma_{\mathbf{k}} (b_{\mathbf{k}}^\dagger c_{-\mathbf{k}}^\dagger + c_{\mathbf{k}}^\dagger a_{-\mathbf{k}}^\dagger) + \text{h.c.} \right]$$

$$+ h(a_{\mathbf{k}}^\dagger a_{\mathbf{k}} + b_{\mathbf{k}}^\dagger b_{\mathbf{k}}) + (2h_0 - h)c_{\mathbf{k}}^\dagger c_{\mathbf{k}}. \quad (3)$$

Here the sum extends over the magnetic Brillouin zone, whose area is 1/3 of the total area of the Brillouin zone, $\gamma_{\mathbf{k}} = J e^{ik_x} + 2J' \cos(\sqrt{3}k_y/2) e^{-ik_x/2}$ and $h_0 = J + 2J'$. The interaction term $H^{(4)} = H_z^{(4)} + H_{\perp}^{(4)}$ is the sum of the transverse (\perp) and longitudinal (z) contributions

$$H_{\perp}^{(4)} = (-\frac{J}{4}) \frac{3}{N} \sum_{\mathbf{k}_1 - \mathbf{k}_3} \{ \gamma_1 (c_1^\dagger a_2^\dagger a_3^\dagger a_{1+2+3} + b_1^\dagger c_2^\dagger c_3^\dagger c_{1+2+3})$$

$$+ a_1^\dagger b_2^\dagger b_3^\dagger b_{1+2+3} + \gamma_{-1} (b_1^\dagger a_2^\dagger a_3^\dagger a_{1+2+3} + a_1^\dagger c_2^\dagger c_3^\dagger c_{1+2+3})$$

$$+ c_1^\dagger b_2^\dagger b_3^\dagger b_{1+2+3} + \text{h.c.} \}, \quad (4)$$

and

$$H_z^{(4)} = \frac{3J}{N} \sum_{\mathbf{k}_1 - \mathbf{k}_3} \{ \gamma_{1-2} a_1^\dagger a_2 b_3^\dagger b_{1-2+3} +$$

$$- \gamma_{1-2} b_1^\dagger b_2 c_3^\dagger c_{1-2+3} - \gamma_{2-1} a_1^\dagger a_2 c_3^\dagger c_{1-2+3} \}. \quad (5)$$

Here we denote for brevity $\gamma_1 \equiv \gamma_{\mathbf{k}_1}$, $a_1 \equiv a_{\mathbf{k}_1}$ and so forth.

If we take only the quadratic part (3) and diagonalize it, we find that the UUD phase is stable for just one field value $h = 3J$ for the isotropic case ($J = J'$) and is unstable for all fields when $\delta \neq 0$. (In the notations which we used in the text, the degree of anisotropy is measure in terms of dimensionless parameter $\delta = (40S/3)(1 - J'/J)^2$, Ref.1). However, interactions between magnons stabilize the UUD phase over the finite δ range. To see this, we first modify the quadratic form by adding the leading $1/S$ Hartree-type self-energy corrections from 4-boson interaction terms (4) and (5), and then diagonalize the effective quadratic Hamiltonian. Since we are interested in large S and small anisotropies (when $\delta = O(1)$) and in field range near $h = 3J$, Hartree corrections can be computed at $\delta = 0$ and $h = 3J$, when classical UUD state is critical and its spin-wave excitation spectrum does not contain complex modes. In 2D Hartree corrections are all finite, and adding them to (3) we obtain the harmonic Hamiltonian of the UUD state in the form

$$H_{\text{uud}} = S \sum_{\mathbf{k}} \left[[\tilde{\gamma}_{1,\mathbf{k}} a_{\mathbf{k}}^\dagger b_{\mathbf{k}} + \tilde{\gamma}_{2,\mathbf{k}} (b_{\mathbf{k}}^\dagger c_{-\mathbf{k}}^\dagger + c_{\mathbf{k}}^\dagger a_{-\mathbf{k}}^\dagger) + \text{h.c.}] + (h + \Sigma_1)(a_{\mathbf{k}}^\dagger a_{\mathbf{k}} + b_{\mathbf{k}}^\dagger b_{\mathbf{k}}) + (2h_0 + \Sigma_2 - h)c_{\mathbf{k}}^\dagger c_{\mathbf{k}} \right] \quad (6)$$

where

$$\tilde{\gamma}_{j,\mathbf{k}} = \gamma_{\mathbf{k}} + \Sigma'_j \quad (7)$$

and the self-energy components are $\Sigma_1 = 0.14J/S$, $\Sigma_2 = 0.67J/S$, $\Sigma'_{1,0} = -0.11J/S$ and $\Sigma'_{2,0} = 0.18J/S$. Observe that (6) reduces to (3) in the $S \rightarrow \infty$ limit.

Alternatively, one could first diagonalize the linear spin-wave part (3), express the 4-boson interaction part in terms of new operators of system's eigen-modes and then correct magnon dispersion by adding to it quadratic terms in new operators, which appear as a result of normal-ordering of Eqs. (4) and (5) in the new basis. Such a procedure was first applied by Oguchi and is known as Oguchi's corrections [2]

Low-energy excitations near $\mathbf{k} = 0$ encode the important physics, and in this region analysis of Eq. (6) simplifies considerably. Here we have $\tilde{\gamma}_{j,\mathbf{k}} \approx \tilde{\gamma}_{j,0} + i\Gamma_{\mathbf{k}}$, with

$$\tilde{\gamma}_{j,\mathbf{k}} = h_0 + \Sigma'_{j,0} - \frac{3}{4}Jk^2, \quad \Gamma_{\mathbf{k}} = (J - J')k_x. \quad (8)$$

Diagonalization of Eq. (6) proceeds in two steps. We first diagonalize H'_{uud} , which is obtained from (6) by setting $\Gamma_{\mathbf{k}} = 0$. This is done by introducing new operators

$$p_{\mathbf{k}} = (a_{\mathbf{k}} - b_{\mathbf{k}})/\sqrt{2}, \quad d_{\mathbf{k}} = (a_{\mathbf{k}} + b_{\mathbf{k}})/\sqrt{2} \quad (9)$$

which decouple in H'_{uud} . However, d -mode couples to c -boson via $\tilde{\gamma}_{j,\mathbf{k}}(d_{\mathbf{k}}^\dagger c_{-\mathbf{k}}^\dagger + \text{h.c.})$ term, and to diagonalize the full quadratic Hamiltonian one needs to apply rotation

$$\begin{aligned} d_{\mathbf{k}} &= \cosh \theta_{\mathbf{k}} u_{\mathbf{k}} + \sinh \theta_{\mathbf{k}} v_{-\mathbf{k}}^\dagger, \\ c_{-\mathbf{k}}^\dagger &= \sinh \theta_{\mathbf{k}} u_{\mathbf{k}} + \cosh \theta_{\mathbf{k}} v_{-\mathbf{k}}^\dagger, \end{aligned} \quad (10)$$

where

$$\tanh(2\theta_{\mathbf{k}}) = \frac{-2\sqrt{2}\tilde{\gamma}_{2,\mathbf{k}}}{2h_0 + \Sigma_1 + \Sigma_2 + \tilde{\gamma}_{1,\mathbf{k}}} \rightarrow -\frac{2\sqrt{2}}{3}. \quad (11)$$

The quadratic Hamiltonian in terms of $u_{\mathbf{k}}$, $v_{\mathbf{k}}$ and $p_{\mathbf{k}}$ operators is

$$H'_{\text{uud}} = S \sum_{\mathbf{k}} [\omega_p p_{\mathbf{k}}^\dagger p_{\mathbf{k}} + \omega_v v_{\mathbf{k}}^\dagger v_{\mathbf{k}} + \omega_u u_{\mathbf{k}}^\dagger u_{\mathbf{k}}]. \quad (12)$$

The u boson describes the precession of the total magnetization. The corresponding frequency $\omega_u(\mathbf{0}) \sim h$ is large, which implies that this mode is irrelevant for low-energy physics. The two remaining bosons, p and v , are the low-energy modes of interest. For small \mathbf{k}

$$\begin{aligned} \omega_p(\mathbf{k}) &= [h - h_{c1}^0 + 2(J - J')] + \frac{3}{4}Jk^2, \\ \omega_v(\mathbf{k}) &\approx [h_{c2}^0 - 2(J - J') - h] + \frac{9}{4}Jk^2. \end{aligned} \quad (13)$$

where $h_{c1}^0 = 3J - 0.5J/(2S)$ and $h_{c2}^0 = 3J + 1.3J/(2S)$ are the boundaries of the UUD phase in the isotropic case.

The next step is to account for the remaining part of H_{uud} in (6), which is proportional to $\Gamma_{\mathbf{k}} = (J - J')k_x$. The corresponding term, which we denote by H''_{uud} , has the form

$$H''_{\text{uud}} = 3iS \sum_{\mathbf{k}} \Gamma_{\mathbf{k}} (p_{\mathbf{k}} v_{-\mathbf{k}} - \text{h.c.}), \quad (14)$$

The diagonalization of $H'_{\text{uud}} + H''_{\text{uud}}$ proceeds in the same way as before: we introduce new operators $d_{1,\mathbf{k}}$ and $d_{2,\mathbf{k}}$ as

$$\begin{aligned} p_{\mathbf{k}} &= \cosh \phi_{\mathbf{k}} d_{1,\mathbf{k}} + i \sinh \phi_{\mathbf{k}} d_{2,-\mathbf{k}}^\dagger, \\ v_{-\mathbf{k}} &= \cosh \phi_{\mathbf{k}} d_{2,-\mathbf{k}} + i \sinh \phi_{\mathbf{k}} d_{1,\mathbf{k}}^\dagger, \end{aligned} \quad (15)$$

and choose $\phi_{\mathbf{k}}$ to eliminate non-diagonal $d_{1,\mathbf{k}} d_{2,-\mathbf{k}}$ terms. This last requirements leads to

$$\tanh(2\phi_{\mathbf{k}}) = \frac{6(J - J')k_x}{\omega_p(\mathbf{k}) + \omega_v(\mathbf{k})} = \frac{6(J - J')k_x}{\Delta h + 3J(k_x^2 + k_y^2)}. \quad (16)$$

Here $\Delta h = h_{c2}^0 - h_{c1}^0 = 1.8J/(2S)$ is the width of the UUD phase at $J' = J$. The diagonalized quadratic Hamiltonian is, up to a constant,

$$H_{\text{uud}} = S \sum_{\mathbf{k}} [\omega_1 d_{1,\mathbf{k}}^\dagger d_{1,\mathbf{k}} + \omega_2 d_{2,\mathbf{k}}^\dagger d_{2,\mathbf{k}}], \quad (17)$$

where at small \mathbf{k}

$$\begin{aligned} \omega_{1,2}(\mathbf{k}) &= \pm \frac{1}{2}(\omega_p - \omega_v) + \frac{1}{2}\sqrt{(\omega_p + \omega_v)^2 - 36(J - J')^2 k_x^2} \\ &= \pm \left(h - h_0 - \frac{1}{5S}J - \frac{3}{4}Jk^2 \right) + \frac{3JZ_{\mathbf{k}}}{20S}, \end{aligned} \quad (18)$$

with $Z_{\mathbf{k}} = \sqrt{9 + 10S(6k^2 - 3\delta k_x^2 + 10S\mathbf{k}^4)}$.

The UUD phase is stable with respect to small perturbations when both modes are positive. The full analysis has been done

in Ref. 1, where it was shown that UUD phase survives up to $\delta = 4$. For our purposes, we focus on the region near the end point. The UUD phase is stable at $h_{c2} > h > h_{c1}$, where

$$h_{c1} = h_{\text{end}} - \frac{27J}{40S} \sqrt{\frac{4-\delta}{3}}, h_{c2} = h_{\text{end}} + \frac{27J}{40S} \sqrt{\frac{4-\delta}{3}}, \quad (19)$$

and $h_{\text{end}} = h_0(1 + 17/120S)$. Near the lower critical field h_{c1} , the mode $\omega_1(k)$ softens at $\pm \mathbf{k}_1 = (k_1, 0)$, where $k_1 \approx (3/(10S))^{1/2}(1 + \sqrt{(4-\delta)/12})$. Near the upper critical field h_{c2} , the mode $\omega_2(k)$ softens at $\pm \mathbf{k}_2 = (k_2, 0)$, where $k_2 \approx (3/(10S))^{1/2}(1 - \sqrt{(4-\delta)/12})$. At $\delta = 4$, the two critical fields become equal $h_{c1} = h_{c2} = h_{\text{end}}$, and both modes soften at the same $k_1^2 = k_2^2 = k_0^2 = 3/(10S)$. At this δ , the excitation spectra are

$$\begin{aligned} \omega_1(k) &= \frac{3J}{2} \sqrt{(k_x^2 - k_0^2)^2 + 4k_0^2 k_y^2} - \frac{3J}{4} (k_x^2 - k_0^2) \\ \omega_2(k) &= \frac{3J}{2} \sqrt{(k_x^2 - k_0^2)^2 + 4k_0^2 k_y^2} + \frac{3J}{4} (k_x^2 - k_0^2) \end{aligned} \quad (20)$$

Observe that at this point $6(J - J')k_0 = 18J/(10S) = 2\Delta h$ and $3Jk_0^2 = \Delta h$, hence $\tanh(2\phi_{k_0,0}) = 1$ in (16), i.e., $\phi_{\mathbf{k}}$ diverges at $\pm \mathbf{k}_0 = (k_0, 0)$. The divergence of ϕ implies that the coherence factors $\cosh \phi_k$ and $\sinh \phi_k$ strongly diverge too. At small deviations from $\pm \mathbf{k}_0$ and $\delta = 4$,

$$\begin{aligned} \cosh 2\phi_{\mathbf{k}} &\approx \sinh 2\phi_{\mathbf{k}} = \frac{1}{2} e^{2\phi_{\mathbf{k}}} \\ &= \frac{2k_0^2}{\sqrt{(k_x^2 - k_0^2)^2 + 4k_0^2 k_y^2 + (4-\delta)k_0^4}} = f^2(k) \end{aligned} \quad (21)$$

Below we will need to express bosons a, b, c via the low-energy eigen-modes d_1 and d_2 . Working backward through transformations (9), (10), and (15), we obtain

$$\begin{aligned} a_{\mathbf{k}} &= \frac{1}{\sqrt{2}} \{ (\cosh \phi_{\mathbf{k}} + i \sinh \phi_{\mathbf{k}}) d_{1,\mathbf{k}} - (\cosh \phi_{\mathbf{k}} - i \sinh \phi_{\mathbf{k}}) d_{2,-\mathbf{k}}^\dagger \}, \\ b_{\mathbf{k}} &= \frac{-1}{\sqrt{2}} \{ (\cosh \phi_{\mathbf{k}} - i \sinh \phi_{\mathbf{k}}) d_{1,\mathbf{k}} + (\cosh \phi_{\mathbf{k}} + i \sinh \phi_{\mathbf{k}}) d_{2,-\mathbf{k}}^\dagger \}, \\ c_{\mathbf{k}} &= \sqrt{2} \{ \cosh \phi_{\mathbf{k}} d_{2,\mathbf{k}} - i \sinh \phi_{\mathbf{k}} d_{1,-\mathbf{k}}^\dagger \}. \end{aligned} \quad (22)$$

Near $\mathbf{k} \pm \mathbf{k}_0$ and $\delta = 4$, $\phi_{\mathbf{k}}$ is large, and using (21) one can simplify the transformation to

$$\begin{aligned} a_{\mathbf{k}} &= \frac{f(\mathbf{k})}{\sqrt{2}} (e^{is_{\mathbf{k}}} d_{1,\mathbf{k}} - e^{-is_{\mathbf{k}}} d_{2,-\mathbf{k}}^\dagger), \\ b_{\mathbf{k}} &= -\frac{f(\mathbf{k})}{\sqrt{2}} (e^{-is_{\mathbf{k}}} d_{1,\mathbf{k}} + e^{is_{\mathbf{k}}} d_{2,-\mathbf{k}}^\dagger), \\ c_{\mathbf{k}} &= f(\mathbf{k}) (d_{2,\mathbf{k}} - e^{i2s_{\mathbf{k}}} d_{1,-\mathbf{k}}^\dagger). \end{aligned} \quad (23)$$

Here $s_{\mathbf{k}} = \pi \text{sign}(k_x)/4$.

Derivation of the pairing interaction between d_1 and d_2 magnons

To obtain the interaction between low-energy magnons, one has to express the interaction Hamiltonian $H^{(4)} = H_z^{(4)} + H_\perp^{(4)}$ written in terms of a, b , and c bosons, Eqs. (4) and (5), via d_1 and d_2 operators with the help of Eq. (22), and find which of the generated interaction terms are the strongest. This procedure is straightforward but time-consuming. We analyzed pairing interaction with zero total momentum of the pair and with total momentum $2k_0$. We found that the interaction matrix elements are much stronger for the former case (zero total momentum pairs). The computational procedure is similar in both cases and we present only the details of the derivation of the strongest interaction.

Because $k_0 = (3/(10S))^{1/2}$ is small, we approximate the factors γ_k in Eqs. (4) and (5) by their values at $k = 0$, i.e., approximate γ_k by $\gamma_0 = J + 2J' \approx 3J$. We verified that that keeping the momentum dependence of $\gamma_{\mathbf{k}}$'s only gives rise to irrelevant small corrections.

We assume and then verify that the dominant contribution to magnon pairing comes from momenta near $\pm k_0$. To obtain the pairing vertices with zero total momentum, it is then convenient to introduce pair operators $\Psi_R(\mathbf{q}) = d_{1,\mathbf{k}_0+\mathbf{q}} d_{2,-\mathbf{k}_0-\mathbf{q}}$ and $\Psi_L(\mathbf{q}) = d_{1,-\mathbf{k}_0+\mathbf{q}} d_{2,\mathbf{k}_0-\mathbf{q}}$, where $|\mathbf{q}| \ll k_0$. Expressing $H^{(4)}$ in terms of d_1 and d_2 we find after long but straightforward calculation that the pairing vertex can be expressed as

$$\begin{aligned} \mathcal{H}_{d_1 d_2}^{(4)} &= -\frac{3J}{2} \frac{3}{N} \sum_{\mathbf{q}, \mathbf{p}} \left((1 + \cosh 2\phi_q \cosh 2\phi_p + \sinh 2\phi_q \sinh 2\phi_p) \times (\Psi_R^\dagger(q) \Psi_L(p) + \Psi_L^\dagger(q) \Psi_R(p)) \right. \\ &\quad + (1 + \cosh 2\phi_q \cosh 2\phi_p - \sinh 2\phi_q \sinh 2\phi_p) \\ &\quad \times (\Psi_R^\dagger(q) \Psi_R(p) + \Psi_L^\dagger(q) \Psi_L(p)) + \\ &\quad + (-1 + \cosh 2\phi_q \cosh 2\phi_p + \sinh 2\phi_q \sinh 2\phi_p) \times \\ &\quad \times (\Psi_R^\dagger(q) \Psi_L^\dagger(p) + \text{h.c.}) \\ &\quad + (-1 + \cosh 2\phi_q \cosh 2\phi_p - \sinh 2\phi_q \sinh 2\phi_p) \times \\ &\quad \left. \times (\Psi_R^\dagger(q) \Psi_R^\dagger(p) + \Psi_L^\dagger(q) \Psi_L^\dagger(p) + \text{h.c.}) \right). \end{aligned} \quad (24)$$

We see that there are two types of pairing vertices: the ones with transferred momentum (for a given boson kind) of the order $2k_0$ (these are $\Psi_L \Psi_R$ terms), and the ones with transferred momentum near zero ($\Psi_L \Psi_L$ and $\Psi_R \Psi_R$ terms). For the first set of terms, the vertex contains $\cosh 2\phi_q \cosh 2\phi_p + \sinh 2\phi_q \sinh 2\phi_p$ and diverges at $\delta = 4$ in the limit $\mathbf{p}, \mathbf{q} \rightarrow 0$. For the second set, the vertex contains $\cosh 2\phi_q \cosh 2\phi_p - \sinh 2\phi_q \sinh 2\phi_p$, and the leading divergent terms cancel out. As a result, the vertex with momentum transfer near $2k_0$ is much stronger. Keeping only this vertex and using the asymptotic forms of $\cosh 2\phi_{q/p}$ and $\sinh 2\phi_{q/p}$ from Eq. (21) we

obtain

$$\begin{aligned} \mathcal{H}_{d_1 d_2}^{(4)} &= (3J) \frac{3}{N} \sum_{\mathbf{q}, \mathbf{p}} f^2(q) (\Psi_R(\mathbf{q}) - \Psi_R^\dagger(\mathbf{q})) \\ &\times f^2(p) (\Psi_L(\mathbf{p}) - \Psi_L^\dagger(\mathbf{p})). \end{aligned} \quad (25)$$

Solution of the gap equation

As is customary in superconductivity studies, we add to the Hamiltonian infinitesimally small pairing terms $Q_L = \Phi_{0,L}(q)\Psi_L(q)$, $Q_R = \Phi_{0,R}(q)\Psi_L(q)$ with generally complex $\Phi_{0,L}$ and $\Phi_{0,R}$ and obtain the renormalized $\Phi_L(q)$ and $\Phi_R(q)$ by summing up ladder series of vertex corrections. At the pairing instability, the pairing susceptibility diverges, and the equations for $\Phi_L(q)$ and $\Phi_R(q)$ have solutions even when we set bare $\Phi_{0,L}(q)$ and $\Phi_{0,R}(q)$ to zero.

The diagrams for the fully renormalized $\Phi_L(q)$ and $\Phi_R(q)$ at the instability are shown in Fig. 1. One can easily make sure that the full set of coupled equations for different Φ and Φ^* separates into two independent sets for Φ_L and Φ_R^* and for Φ_R and Φ_L^* . Because the momentum dependence of the pairing vertex in Eq. (25) is factorized into $f^2(p)f^2(q)$, we search for the solution in the form $\Phi_L(q) = \tilde{\Upsilon} f^2(q)$. Substituting this form into the diagrams and using one-magnon dispersions from (20) we obtain after a simple algebra

$$\begin{aligned} \tilde{\Upsilon} &= (\tilde{\Upsilon} - \tilde{\Upsilon}^*) \frac{3}{NS} \sum_p \frac{3Jf^4(p)}{\omega_1(k_0 + p) + \omega_2(k_0 + p)} \\ &= i(\text{Im} \tilde{\Upsilon}) \frac{3}{NS} \sum_p \frac{k_0}{(p^2 + (1 - \delta/4)k_0^2)^{3/2}} \end{aligned} \quad (26)$$

We used the fact that $\omega_1(k_0 + p) + \omega_2(k_0 + p) = 6Jk_0^2/f^2(\mathbf{p})$ (see Eq. (20)). It is obvious from Eq. (26) that $\tilde{\Upsilon}$ should be purely imaginary, $\tilde{\Upsilon} = i\Upsilon$. Substituting this into (26), we find that the equation for Υ has a non-trivial solution when

$$1 = \frac{1}{S} \frac{3}{N} \sum_p \frac{k_0}{|\mathbf{p}|^3} \quad (27)$$

Generalizing this to $\delta \leq 4$ case, and replacing the sum over p by integral we find that the condition on the pairing instability reduces to

$$\int \frac{d^2 p}{(p^2 + (1 - \delta/4)k_0^2)^{3/2}} = \tilde{a} \frac{S}{k_0} \quad (28)$$

where $\tilde{a} = O(1)$. Evaluating the integral we find that the two-magnon instability occurs at $4 - \delta = O(1/S^2)$.

Alternative derivation of Eq. (27).

We start from simple observation that

$$[\mathcal{H}_{\text{udd}}^{(2)}, \Psi_R(\mathbf{q})] = -S \left(\omega_1(\mathbf{k}_0 + \mathbf{q}) + \omega_2(-\mathbf{k}_0 - \mathbf{q}) \right) \Psi_R(\mathbf{q}), \quad (29)$$

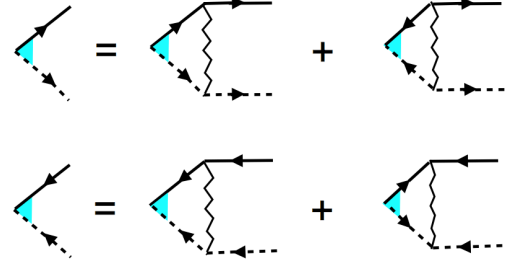


FIG. 1: (Color online) Coupled set of diagrams for anomalous vertices Φ_L (upper line) and Φ_R^* (lower line).

and similarly for $\Psi_L(\mathbf{q})$. We also see that

$$[\Psi_R(\mathbf{q}), \Psi_R^\dagger(\mathbf{p})] = \delta_{q,p} (1 + d_{1,\mathbf{k}_0+\mathbf{q}}^\dagger d_{1,\mathbf{k}_0+\mathbf{q}} + d_{2,\mathbf{k}_0-\mathbf{q}}^\dagger d_{2,\mathbf{k}_0-\mathbf{q}}) \quad (30)$$

and $[\Psi_R(\mathbf{q}), \Psi_L^\dagger(\mathbf{p})] = 0$ because for $q, p \ll k_0$, the two pairs do not overlap in momentum space. Inside the UUD plateau $\langle d_{1/2,\mathbf{k}}^\dagger d_{1/2,\mathbf{k}} \rangle = 0$, where the average is over the ground state. Hence the right-hand side of (30) can be replaced by $\delta_{q,p}$, implying canonical bosonic commutation relations for pairs $\Psi_{R/L}$. This allows for an easy derivation of the equations of motion for pair operators. We obtain

$$\begin{aligned} i\partial_t \Psi_R(\mathbf{k}) &= \Omega_{\mathbf{k}} \Psi_R(\mathbf{k}) - \frac{3}{N} \sum_{\mathbf{p}} \Phi(\mathbf{p}, \mathbf{k}) (\Psi_L^\dagger(\mathbf{p}) - \Psi_L(\mathbf{p})), \\ i\partial_t \Psi_L(\mathbf{k}) &= \Omega_{\mathbf{k}} \Psi_L(\mathbf{k}) - \frac{3}{N} \sum_{\mathbf{p}} \Phi(\mathbf{p}, \mathbf{k}) (\Psi_R^\dagger(\mathbf{p}) - \Psi_R(\mathbf{p})), \\ i\partial_t \Psi_R^\dagger(\mathbf{k}) &= -\Omega_{\mathbf{k}} \Psi_R^\dagger(\mathbf{k}) - \frac{3}{N} \sum_{\mathbf{p}} \Phi(\mathbf{p}, \mathbf{k}) (\Psi_L^\dagger(\mathbf{p}) - \Psi_L(\mathbf{p})), \\ i\partial_t \Psi_L^\dagger(\mathbf{k}) &= -\Omega_{\mathbf{k}} \Psi_L^\dagger(\mathbf{k}) - \frac{3}{N} \sum_{\mathbf{p}} \Phi(\mathbf{p}, \mathbf{k}) (\Psi_R^\dagger(\mathbf{p}) - \Psi_R(\mathbf{p})), \end{aligned} \quad (31)$$

where $\Omega_{\mathbf{k}} = S(\omega_1(\mathbf{k}_0 + \mathbf{q}) + \omega_2(-\mathbf{k}_0 - \mathbf{q}))$ and $\Phi(q, p) \approx -3Jf^2(p)f^2(q)$. We now Fourier transform t -dependence ($i\partial_t \rightarrow \omega$) and set $\omega = 0$ because we are seeking the condition for the pair condensation. We then take expectation values of both sides of equations and form appropriate linear combinations to obtain

$$\begin{aligned} \langle \Psi_R^\dagger(\mathbf{k}) - \Psi_R(\mathbf{k}) \rangle &= \frac{6Jf^2(\mathbf{k})}{\Omega_{\mathbf{k}}} \frac{3}{N} \sum_{\mathbf{p}} f^2(\mathbf{p}) \langle \Psi_L^\dagger(\mathbf{p}) - \Psi_L(\mathbf{p}) \rangle \\ \langle \Psi_L^\dagger(\mathbf{k}) - \Psi_L(\mathbf{k}) \rangle &= \frac{6Jf^2(\mathbf{k})}{\Omega_{\mathbf{k}}} \frac{3}{N} \sum_{\mathbf{p}} f^2(\mathbf{p}) \langle \Psi_R^\dagger(\mathbf{p}) - \Psi_R(\mathbf{p}) \rangle. \end{aligned} \quad (32)$$

where we used $\gamma_k \approx 3J$. We immediately see that Φ_R and Φ_L must be purely imaginary, and $\Phi_{L,R}(k) \propto f^2(k)$. The self-consistency condition then gives

$$\frac{3}{N} \sum_{\mathbf{p}} \frac{6Jf^4(\mathbf{p})}{\Omega_{\mathbf{p}}} = \frac{1}{S} \frac{3}{N} \sum_{\mathbf{p}} \frac{k_0}{|\mathbf{p}|^3} = 1, \quad (33)$$

which is the same condition as Eq. (27).

Pair condensation and spontaneous generation of Dzyaloshinskii-Moria interaction

We first observe that Eq. (25) can be re-written as

$$\mathcal{H}_{d_1 d_2}^{(4)} = -(J + 2J') \frac{3}{N} \mathcal{H}_{+k_0}^{\text{DM}} \mathcal{H}_{-k_0}^{\text{DM}}. \quad (34)$$

where

$$\begin{aligned} \mathcal{H}_{k_0}^{\text{DM}} &= i \sum_{\mathbf{q}} f^2(\mathbf{q}) \left(\Psi_R(\mathbf{q}) - \Psi_R^\dagger(\mathbf{q}) \right), \\ \mathcal{H}_{-k_0}^{\text{DM}} &= i \sum_{\mathbf{q}} f^2(\mathbf{q}) \left(\Psi_L(\mathbf{q}) - \Psi_L^\dagger(\mathbf{q}) \right). \end{aligned} \quad (35)$$

Note that the integrands in (35) is the same as the two-magnon order parameter

$$i \sum_{\mathbf{q} \in \pm \mathbf{k}_0} f^2(\mathbf{q}) \left(d_{1,\mathbf{q}} d_{2,-\mathbf{q}} - d_{1,\mathbf{q}}^\dagger d_{2,-\mathbf{q}}^\dagger \right). \quad (36)$$

Hence, once two-magnon condensation occurs, $\langle \mathcal{H}_{\pm k_0}^{\text{DM}} \rangle$ acquires a non-zero expectation value, proportional to Υ , i.e., the Hamiltonian acquires an extra term

$$\mathcal{H}_{d_1 d_2}^{(4)} = D [\mathcal{H}_{+k_0}^{\text{DM}} + \mathcal{H}_{-k_0}^{\text{DM}}]. \quad (37)$$

where

$$D = -(J + 2J') \frac{3}{N} \langle \mathcal{H}_{+k_0}^{\text{DM}} \rangle = (J + 2J') \Upsilon. \quad (38)$$

(See next section for a very similar calculation.) We now compare the Hamiltonian in Eq. (37) with the one which describes Dzyaloshinskii-Moria (DM) interaction in a triangular magnet and show that they are identical. The DM interaction on a triangular lattice reads [3]

$$\begin{aligned} H_{\text{DM-latt}} &= \hat{z} \cdot \sum_{\mathbf{r}} \left(\mathbf{S}_C(\mathbf{r}) \times \mathbf{S}_B(\mathbf{r}) + \mathbf{S}_A(\mathbf{r}) \times \mathbf{S}_C(\mathbf{r}) + \right. \\ &\quad \left. + \mathbf{S}_B(\mathbf{r}) \times \mathbf{S}_C(\mathbf{r}) \right). \end{aligned} \quad (39)$$

In our case z coincides with the direction of external field. Expressing the spins in terms of Holstein-Primakoff bosons a, b , and c and transforming to d_1 and d_2 operators using (23) we obtain that after some algebra (22) gives

$$H_{\text{DM-latt}} = 6S(\mathcal{H}_{+k_0}^{\text{DM}} + \mathcal{H}_{-k_0}^{\text{DM}}). \quad (40)$$

Comparing with (37) we immediately see that the appearance of a two-magnon condensate with an imaginary amplitude Υ can be viewed as a spontaneous generation of DM interaction with the coupling $D \propto \Upsilon$.

Structure of spin currents

The z -component of the spin current on the bond $\langle n, m \rangle$, connecting sites n and m , is defined as

$$J_{nm}^z = \frac{1}{2i} (S_n^- S_m^+ - S_n^+ S_m^-). \quad (41)$$

Re-expressing the r.h.s. of this expression in terms of a, b , and c bosons, we find that spin currents along the bonds between spins from A, B, and C sublattices belonging to the same elementary triangle at a coordinate r are determined by the following combinations

$$\begin{aligned} J_{CA}^z &= iS(c_{\mathbf{r}}^+ a_{\mathbf{r}}^+ - c_{\mathbf{r}} a_{\mathbf{r}}), \quad J_{CB}^z = iS(c_{\mathbf{r}}^+ b_{\mathbf{r}}^+ - c_{\mathbf{r}} b_{\mathbf{r}}), \\ J_{AB}^z &= iS(b_{\mathbf{r}}^+ a_{\mathbf{r}} - a_{\mathbf{r}}^+ b_{\mathbf{r}}). \end{aligned} \quad (42)$$

Using (23), we obtain

$$\begin{aligned} \langle c_{\mathbf{r}} a_{\mathbf{r}} \rangle &= \frac{3}{\sqrt{2}N} \sum_{\mathbf{k}, \mathbf{q}} e^{i\mathbf{r} \cdot (\mathbf{k} + \mathbf{q})} f(\mathbf{k}) f(\mathbf{q}) \langle (d_{2,\mathbf{k}} - e^{i2s_{\mathbf{k}}} d_{1,-\mathbf{k}}^\dagger) \\ &\quad \times (e^{is_{\mathbf{q}}} d_{1,\mathbf{q}} - e^{-is_{\mathbf{q}}} d_{2,-\mathbf{q}}^\dagger) \rangle. \end{aligned} \quad (43)$$

The condensate emerges at $\mathbf{q} = -\mathbf{k}$, and we obtain

$$\begin{aligned} \langle c_{\mathbf{r}} a_{\mathbf{r}} \rangle &= \frac{3}{\sqrt{2}N} \sum_{\mathbf{k}} f^2(\mathbf{k}) e^{-is_{\mathbf{k}}} \langle d_{1,-\mathbf{k}} d_{2,\mathbf{k}} - d_{1,-\mathbf{k}}^\dagger d_{2,\mathbf{k}}^\dagger \rangle \\ &= \frac{3}{\sqrt{2}N} \sum_{\mathbf{k}} f^2(\mathbf{k}) e^{-is_{\mathbf{k}}} (2i\Upsilon) \frac{3Jf^2(\mathbf{k})}{S(\omega_1 + \omega_2)} \\ &= \frac{i\Upsilon}{S k_0^2} \frac{3}{N} \sum_{\tilde{\mathbf{k}}} \left(\frac{k_0^2}{\tilde{k}_x^2 + \tilde{k}_y^2 + (1 - \delta/4)k_0^2} \right)^{3/2} \\ &= i\Upsilon. \end{aligned} \quad (44)$$

Here \tilde{k} is the deviation from $\pm \mathbf{k}_0$, near which the phase factor takes values $s_{\mathbf{k}} = \pm \pi/4$ correspondingly. The last line in the above equation is a direct consequence of the linearized “gap” equation (10) of the main text (which, of course, is the same as (26) and (27) of Supplementary Material), to which the right-hand-side of (44) reduces.

Because $\langle c_{\mathbf{r}} a_{\mathbf{r}} \rangle$ is imaginary, it does not contribute to $\mathbf{S}_C \cdot \mathbf{S}_A \propto \text{Re}(S_C^+ S_A^-)$, but the spin current J_{CA}^z becomes non-zero. Similar calculation for other bonds that $\langle c_{\mathbf{r}} a_{\mathbf{r}} \rangle = -\langle c_{\mathbf{r}} b_{\mathbf{r}} \rangle = \langle a_{\mathbf{r}}^\dagger b_{\mathbf{r}} \rangle$. These relations fix the relative signs of spin currents and lead to two current patterns shown in Figure 2 of the main text.

It is easy to generalize this calculation for the spins located at distance \mathbf{R} apart from each other (we assume that $R \gg k_0^{-1}$)

$$\begin{aligned} \langle \hat{z} \cdot \mathbf{S}_C(\mathbf{R}) \times \mathbf{S}_A(0) \rangle &\propto S \text{Im} \langle c_{\mathbf{R}} a_0 \rangle \\ &\sim \Upsilon k_0 \cos[\mathbf{k}_0 \cdot \mathbf{R}] \int_0^\infty d\tilde{k} \int_0^{2\pi} d\phi \frac{\tilde{k} e^{i\mathbf{k} \cdot \mathbf{R} \cos[\phi]}}{(\tilde{k}^2 + (1 - \delta/4)k_0^2)^{3/2}} \\ &\sim \Upsilon k_0 \cos[\mathbf{k}_0 \cdot \mathbf{R}] \int_0^\infty d\tilde{k} \frac{\tilde{k} J_0(\tilde{k} R)}{(\tilde{k}^2 + (1 - \delta/4)k_0^2)^{3/2}} \\ &= \Upsilon k_0 \cos[\mathbf{k}_0 \cdot \mathbf{R}] \xi e^{-R/\xi}, \end{aligned} \quad (45)$$

where J_0 is the Bessel function and $\xi^{-1} = k_0 \sqrt{1 - \delta/4}$. The correlation decays exponentially for $R \gg \xi$. This implies that ξ has the meaning of the radius of a two-magnon bound state. Using the relation $\delta_{\text{cr}} = 4 - O(1/S^2)$, we obtain $\xi \sim S/k_0$.

[2] T. Oguchi, Phys. Rev. **117**, 117 (1960).

[3] C. Griset, S. Head, J. Alicea, O. A. Starykh, Phys. Rev. B **84**, 245108 (2011).

[1] J. Alicea, A. V. Chubukov, and O. A. Starykh, Phys. Rev. Lett. **102**, 137201 (2009).